CORRELATION OF NEAR-EARTH PROTON ENHANCEMENTS >100 MeV WITH PARAMETERS OF SOLAR MICROWAVE BURSTS

V.V. Grechnev
Institute of Solar-Terrestrial Physics SB RAS,
Irkutsk, Russia, grechnev@iszf.irk.ru

V.I. Kiselev
Institute of Solar-Terrestrial Physics SB RAS,
Irkutsk, Russia, valentin_kiselev@iszf.irk.ru

N.S. Meshalkina
Institute of Solar-Terrestrial Physics SB RAS,
Irkutsk, Russia, nata@iszf.irk.ru

I.M. Chertok
Pushkov Institute of Terrestrial Magnetism, Ionosphere and
Radio Wave Propagation RAS,
Troitsk, Moscow, Russia, ichertok@izmiran.ru

Abstract. We analyze the relations between various combinations of peak fluxes and fluences of solar microwave bursts at 35 GHz recorded with the Nobeyama Radio Polarimeters during 1990–2015, and corresponding parameters of proton enhancements with $E>100$ MeV exceeding 0.1 pfu registered by GOES monitors in near-Earth environment. The highest correlation has been found between the microwave and proton fluences. This fact reflects a dependence of the total number of protons on the total duration of the acceleration process. In the events with strong flares, the correlation coefficients of proton fluences with microwave and soft X-ray fluences are higher than those with speeds of coronal mass ejections. The results indicate a statistically larger contribution of flare processes to acceleration of high-energy protons. Acceleration by shock waves seems to be less important at high energies in events associated with strong flares, although its contribution probably prevails in weaker events. The probability of a detectable proton enhancement was found to directly depend on the peak flux and duration of a microwave burst. This can be used for diagnostics of proton enhancements based on microwave observations.

Keywords: proton events, solar flares, radio radiation.

INTRODUCTION

The problems of the origin of solar proton events (SPEs) and their diagnostics have been actively discussed for almost half a century [Bazilevskaya, 2009; Miroshnichenko et al., 2013]. Space weather disturbances caused by solar activity can pose a threat to various branches of human activity and to human health. High-energy particle fluxes are dangerous for both spacecraft crews and equipment. The first mission, which arrived at the International Space Station on 2000 November 2, was exposed to the most powerful SPE on November 8–10 (see, e.g., [Lario et al., 2009, Logachev et al., 2016]). Secondary particles produced by solar cosmic rays (SCR) in Earth's atmosphere can also give noticeable radiation doses to crew members and passengers of transcontinental flights passing high-latitude regions. The extreme solar activity outburst at the end of 2003 October forced a change in the transcontinental routes during that period [Veselovsky et al., 2004].

Particles can be accelerated by flare processes in an active region or by shock waves in a larger space [Cliver et al., 1989; Kallenrode, 2003; Aschwanden, 2012; Reames, 2013; Desai, Giacalone, 2016]. These two possible acceleration sites are assumed to be remote and virtually independent of each other. The main accelerator of protons, which reach the Earth orbit, is widely believed to be bow shocks driven by super-Alfvénic coronal mass ejections (CME) in the high corona [Reames, 2009, 2013; Gopalswamy et al., 2014]. This concept seems to be supported by results of the velocity dispersion analysis for solar particles with different energies. This analysis shows that the extrapolated time of particle escape near the Sun into the interplanetary space is delayed relative to a flare. This is considered as an argument for their acceleration by CME-driven bow shocks. Proceeding from the hypothesis about the bow-shock excitation scenario, its proponents compare SPE properties with observable manifestations corresponding to those suggested by this hypothesis. For example, the onset of a type II radio burst is considered to be an indicator of the shock formation corresponding to the transition of the CME leading edge to the super-Alfvénic regime. Basing on these assumptions, researchers are attempting to associate properties of the shock wave responsible for proton acceleration with the initial frequency of the type II radio burst.

However, this correspondence is not expected either for another (for example, impulsive-piston) shock-wave excitation mechanism or for the location of the type II burst source on a flank of the shock. We have established a closer (than previously thought) relation between evolution of eruptive flares and excitation of shock waves [Grechnev et al., 2013a, 2015b]. Thus, the traditional contrast between shock-related and flare-related acceleration of particles may not be fully justified.

Earlier studies point out that parameters of solar energetic particles correlate with those of microwave bursts [Croom, 1971, Akinyan et al., 1978]. Yet, Kahler [1982] attributes this correlation to the "Big Flare Syndrome", i.e. a general correspondence between the energy release in an eruptive flare and its various manifestations regardless of any physical connection between

them. Subsequently, the exaggeration of the shock-related acceleration led to underestimation of diagnostic capabilities of microwave bursts. Nevertheless, a number of studies conclude that flare processes play an essential role in accelerating SCR and confirm that the diagnostics of SPEs from flare radio emission is promising [Daibog et al., 1987; Chertok, 1990; Melnikov et al., 1991; Isaeva et al., 2010]. In this respect, the correlation might be important between the parameters of the frequency spectrum of microwave bursts and the energy spectrum of near-Earth proton fluxes [Chertok et al., 2009]. In [Grechnev et al., 2008; Klein et al., 2014], the authors argue that the flare-related acceleration dominated in the 2005 January 20 extreme SPE. Grechnev et al. [2013b, 2015a] show that contrasting of sources of accelerated protons in different extreme events is not justified. A shock wave appearing during a flare can accelerate particles much earlier than the CME speed exceeds the Alfvén velocity. Flare-accelerated particles trapped in a CME flux rope can be released only after its reconnection with an open magnetic structure. Hence, the delayed escape of accelerated particles into the interplanetary space suggests their acceleration by the flare, rather than by the shock wave. This reverses the conclusion derived from the velocity dispersion analysis. Thus, recent results indicate that the analysis of the relationships between microwave bursts and proton enhancements is useful irrespective of SPE origin.

We analyze relationships between flare and CME parameters and high-energy SPEs to determine the contribution of the two possible sources of particle acceleration. The main goals are to find the highest correlation between parameters of solar eruptive events and SPEs and to identify possible patterns for prompt diagnostics of SPE from microwave observations.

Section 1 summarizes our previously obtained statistical results (1.1), lists data sources, characterizes their selection and processing (1.2). Section 2 analyzes dependences of SPE probability on the intensity of a microwave burst (2.1) and its duration (2.2), compares correlations between different combinations of peak microwave fluxes and fluences and those of proton enhancements (2.3). Section 3 examines the relationships between different parameters of solar eruptive activity and proton fluences. Section 4 discusses the results.

1. PRELIMINARY RESULTS AND DATA PROCESSING

1.1. Earlier results

The gyrosynchrotron emission of accelerated electrons observed as microwave bursts depends on their parameters and on the magnetic field in the source and its dimensions. These dependences differ significantly for the optically thick regime (below the frequency of the spectral peak of the gyrosynchrotron emission) and for the optically thin regime (at frequencies above the spectral peak). The microwave emission in the optically thin regime is the most sensitive to high-energy electrons and is most directly related to the rate of energy release in the flare–CME process. The frequency of the

spectral peak also depends on the above parameters. Therefore, microwave data at a fixed frequency are ambiguous, referring to the region of the gyrosynchrotron emission spectrum to the left of the peak in some events and to the right of it in the others. To minimize this ambiguity, it is reasonable to analyze microwave data at the highest possible frequency. The highest frequency at which stable long-term measurements of the total solar radio flux are made is 35 GHz. These observations have been carried out with Nobeyama Radio Polarimeters (NoRP) [Nakajima et al., 1985]) since 1990.

Grechnev et al. [2013b] have analyzed the relationships between peak microwave fluxes ≥ 1000 sfu (1 sfu = 10^{-22} W m^{-2} Hz^{-1}) at 35 GHz (F_{35}) and peak proton fluxes with energies above 100 MeV (J_{100}) for 1990–2012. For the analysis to be complete, the authors identified and examined events for the same period, which caused SPEs $J_{100}>10$ pfu (1 pfu = 1 cm^{-2}s^{-1}sr^{-1}) associated with weaker microwave bursts. The full list comprises 98 events. For convenience, categories of the events were introduced by analogy with the GOES classification. These categories were determined from the peak microwave flux at 35 GHz: $F_{35}>10^4$ sfu – mX (microwave-Extreme), 10^3 sfu $< F_{35}<10^4$ sfu – mS (microwave-Strong), $F_{35}<10^3$ sfu – mM (microwave-Moderate) and mO (microwave-Occulted) – for the events behind the solar limb whose emission is not observable from Earth.

Four groups of events have been identified:

1) events with a trend between proton fluxes as microwave fluxes – the group to which most events belong;

2) events with intense bursts at 35 GHz without proton enhancements, detectable in the GOES integral proton channel above 100 MeV;

3) atypically abundant SPEs after moderate microwave bursts (mM) – few events;

4) SPEs associated with the occulted sources (mO) – few events.

A preliminary diagnostic criterion has been formulated: if an event occurs in the visible part of the western solar hemisphere and is accompanied by a significant microwave burst, CME, and type II burst, one can expect an enhancement of near-Earth proton flux J_{100}, expressed in pfu, ranging from $(F_{35}/1100)^2$ to $(F_{35}/13000)^2$, where F_{35} is expressed in sfu. If a microwave burst is very strong, then significant SPE can occur even when a solar source is located in the eastern hemisphere, especially if the burst has a long duration. It has been established that high-energy SPEs feature flare ribbons above sunspot umbras. This is consistent with the presence of powerful microwave bursts in these events caused by the gyrosynchrotron emission in strong magnetic fields of numerous high-energy electrons [Grechnev et al., 2008].

Grechnev et al. [2015a] continued analyzing the selected events. The list was expanded to 111 events. The authors studied relationships between various combinations of peak microwave fluxes and fluences (integrated over the time of emission fluxes) at 35 GHz and proton enhancements with energies >100 MeV. They used the detailed time histories and spectra

of both the proton enhancements in Earth's orbit and the microwave burst in its solar source, and the location of the source on the Sun. To make the picture complete and to verify the previously obtained results and assumptions, we expand the list of events to 2015 March and supplement it with much weaker SPEs (0.1 pfu < J_{100} < 10 pfu) observed since 1996.

1.2. Data

The data list of microwave bursts recorded by NoRP is available on the website [http://solar.nro.nao.ac.jp/ norp/html/event]. The data on bursts at 35 GHz cover the period from 1990 April 15 to 2015 March 10. We have analyzed all events from this list with peak fluxes at 35 GHz above 1000 sfu ($F_{35} \geq 10^3$); 104 events satisfy this criterion. Correlations of SPEs with CME parameters can be analyzed starting from 1996, when LASCO observations began. To take account of SPEs after weaker microwave bursts, we also examined all proton enhancements occurring since 1996, whose peak fluxes met the condition $J_{100} \geq 0.1$ pfu, and the respective microwave bursts fell into the observing time in Nobeyama.

These SPEs have been selected from the archive containing standard three-day plots of proton fluxes recorded by monitors onboard GOES satellites in three integral channels between 1996 and March 2015 [ftp://ftp.swpc.noaa.gov/pub/warehouse]. Extensive additional information is present in a number of articles and catalogs of SPEs, including electronic [Sladkova et al., 1998; Kurt et al., 2004; Veselovsky et al., 2012; Logachev et al., 2016; http://www.wdcb.ru/stp/data/ SPE]. As a result, we additionally found 34 events. In subsequent selection, we identified the solar source of an event from movies and sets of images obtained with the Nobeyama Radioheliograph [http://solar.nro.nao.ac.jp/ norh], extreme ultraviolet imaging telescopes and coronagraphs aboard SOHO [http://cdaw.gsfc.nasa.gov/ CME_list; http://lasco-www.nrl.navy.mil/daily_mpg], STEREO [http://cdaw.gsfc.nasa.gov/stereo/daily_ movies], and SDO [http://sdo.gsfc.nasa.gov/data/ aiahmi] for respective periods.
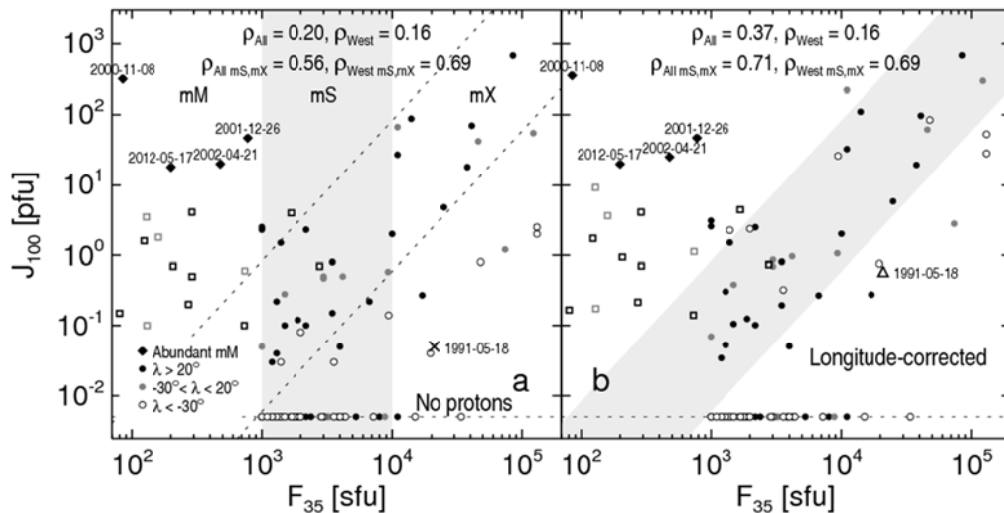

Figure 1. Relationship between peak SPE fluxes E_p>100 MeV and bursts at 35 GHz: actual values (*a*), with longitude correction (*b*). The longitude of a solar source is represented by symbols: open circles are distant eastern events (λ<–30°), black circles are western events (λ>20°), gray circles are events in –30°<λ<20°. Squares indicate 13 mM events with 0.1≤J_{100}<10 pfu: black squares are western events, gray squares are those in –30°<λ<20°. Black diamonds are four atypical proton-abundant mM events. Events without detectable proton enhancements are shown on the horizontal dotted line. The Pearson correlation coefficients calculated for all the events and separately for the western ones are indicated at the top. The correlation coefficients with mS, mX indices are computed for corresponding categories of events. Slanted dashed lines (F_{35}/13 000)^2 and (F_{35}/1100)^2 in panel (*a*) mark boundaries of the shaded area in panel (*b*). These lines bound the main cloud of points and indicate the direct correspondence between F_{35} and J_{100}

Sixteen events were associated with the behind-the-limb sources whose microwave emission could not reach Earth. It is difficult to draw any conclusions for these events; therefore, they are excluded from further consideration. We also omit events for which GOES or NoRP data are unsatisfactory. A complete set of events (121 events, including 13 events with peak SPE fluxes $J_{100} \geq 0.1$ pfu and weak microwave bursts) is listed in the Table at [http://iszf.irk.ru/~grechnev/papers/protons_ microwaves/Table.htm]. The Table structure is the same as in [Grechnev et al., 2015a], but it is supplemented with a column of proton fluences in the rise phase. Events in the Table are arranged in descending

order of their categories – mX, mS, and mM respectively. Within each category, the order is chronological. The mO events are not included in the Table and are not analyzed.

Automatically processed digital NoRP data in XDR format (IDLsave) are available at [ftp://solar-pub.nao. ac.jp/pub/nsro/norp/xdr]. The method for additional, more accurate processing of NoRP data and estimation of quantitative parameters of bursts is presented in [Grechnev et al., 2013b]. For all the events, we refined and subtracted pre-burst microwave emission levels because the accuracy of their evaluation by software in Nobeyama is often insufficient. The contribution of the

gyrosynchrotron emission of accelerated electrons in the bursts with $F_{35}<10^3$ sfu was eliminated by subtracting from microwave profiles thermal bremsstrahlung calculated from GOES soft X-ray (SXR) data by a standard procedure. This contribution is insignificant for stronger bursts. We have revealed and fixed inconsistency in our previous measurements of burst durations, which appeared in the transition from initial estimates of their total duration to subsequent half-level measurements; this inconsistency distorted the quantitative results of the analysis in [Grechnev et al., 2015a]. The microwave burst durations listed in the Table and analyzed in this study were measured uniformly at the half level.

Digital data from GOES proton monitors are available at http://satdat.ngdc.noaa.gov/sem/goes/data/new_avg. Total proton fluences were calculated for the integral proton channel $E_p>100$ MeV with the background level subtracted for the entire time of proton enhancement. Proton fluences during the rise phase were computed in a similar way. If SPE overlapped with the decay of a preceding event, then the background was fit with an exponential function.

The analyzed dataset is shown in Figure 1, *a*, similar to a corresponding Figure in [Grechnev et al., 2013b]. The Figure presents the relationships between peak proton fluxes with $E_p>100$ MeV and microwave bursts at 35 GHz. Solar source events are categorized according to their heliolongitude λ into three intervals with boundaries of –30° and +20°. The longitude ranges are represented by grayscale. Events without proton enhancements are schematically shown on the horizontal dotted line at the bottom. Most SPEs fall between slanted lines, forming the main sequence. Four atypical proton-abundant mM events (black squares located much higher than the main sequence in the left part of the plot): 2000-11-08, 2001-12-26, 2002-04-21, 2012-05-17 – occurred after moderate microwave bursts with $F_{35}<10^3$ sfu. Two of them caused ground-level enhancements of cosmic-ray intensity (GLEs): 2001-12-26 (GLE63) and 2012-05-17 (GLE71). The 1991-05-18 SPE (marked with the cross in panel *a* and with the triangle in panel *b*) is associated with the western source, but in its properties this event looks like a typical SPE from an eastern source. Therefore, the event is considered to have the longitude of E45 [Grechnev et al., 2015a]. The correlation coefficients between logarithms of peak values of microwave and proton fluxes for all the events (ρ_{All}) and separately for events in the western hemisphere with heliolongitudes λ>20° (ρ_{West}) are given at the top. Hereafter, we call the events in the western hemisphere western events and those in the eastern hemisphere eastern events. The correlation for western events is lower because of the larger contribution from the four atypical mM events.

Figure 1, *b* shows the same events but with a correction of proton fluxes for the longitudinal dependence in propagation of >100 MeV protons: $\exp([(λ- 54°)/63]^2)$ [Belov et al., 2009]. This dependence is similar to that obtained in [Lario et al., 2013] for 25–53 MeV protons. An analogous approach has been used before, for example in [Kahler, 1982]. The longitudinal correction increases the correlation for the entire ensemble of events by 70 %. It was applied to all parameters of SPEs, including those with western sources. Since this correction is not undoubted, correlation coefficients were also calculated separately for western events. Note that these correlation coefficients and regression parameters refer to logarithms of the analyzed quantities, rather than to actual values because of their wide dynamic range. The results of application of linear statistical methods on the log scale are not correct. Well-known alternative methods absent, we have to use this approach, which is employed in almost all similar studies (see, e.g., [Kahler, 1982, Trottet et al., 2015, Dierckxsens et al., 2015], etc.) as a compromise, being aware that the results are not mathematically rigorous.

2. RELATIONSHIPS BETWEEN PARAMETERS OF MICROWAVE BURSTS AND SPEs

2.1. Probability of proton events versus 35 GHz burst intensity

Figure 2 shows the distribution of > 100 MeV SPE probability versus the peak microwave flux at 35 GHz (F_{35}).
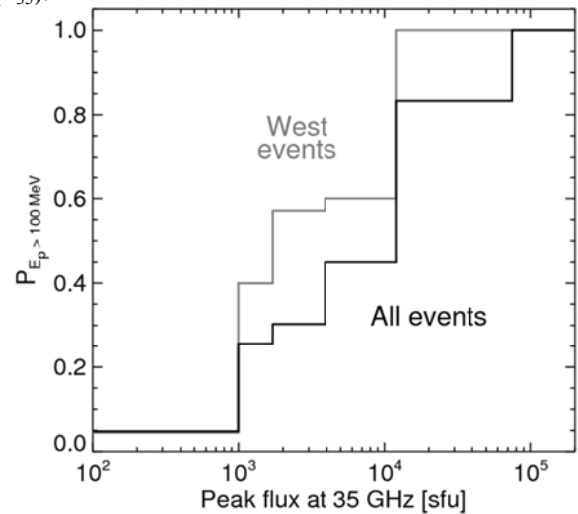

Figure 2. Probability of SPEs with $E_p>100$ MeV versus the peak microwave flux at 35 GHz irrespective of its duration and solar source location. The gray histogram corresponds to western events; the black histogram, to all events

The shape of the histogram is sensitive to the bins because of a relatively small number of events. We have chosen the bins to reach their possibly larger number, keeping the histogram monotonic. With the peak microwave flux $F_{35}≈10^3$ sfu, the probability of SPEs is about 35 %. With increasing F_{35}, the probability increases, approaching 100 % at $F_{35}≥10^5$ sfu. The SPE probability after a western solar event is 10–20 % higher than that averaged over the whole set of events.

Thus, the probability of a SPE directly depends on the peak flux of a microwave burst at 35 GHz. This fact is consistent with the conclusion drawn by Grechnev et al. [2013b, 2015a] that powerful microwave

bursts indicate large SPEs.

2.2. The role of burst duration

Events without SPEs are schematically shown on the horizontal dotted line at the bottom of Figure 1. The half-height durations of the corresponding microwave bursts range from 0.06 to 18.8 min with an average of 2.3 min (σ_n = 2.5 min). The burst durations in proton events range from 0.23 to 68 min with an average of 7.7 min (σ_p = 7.9 min). The average durations differ by a factor of 3.3. For the analysis we use the integral probability distribution $P(\Delta t \leq t)$ characterizing the probability of an event if its duration Δt does not exceed t.

In Figure 3, a, the solid line represents the integral probability distribution for microwave bursts depending on their duration for events that caused SPEs. The shape of this distribution is close to exponential:

$$P(\Delta t \leq t)=1-\exp(-t/\tau).$$

Its derivative is the probability density distribution and has the form $\exp(-t/\tau)/\tau$. Minimizing the difference between the actual distribution and its analytical
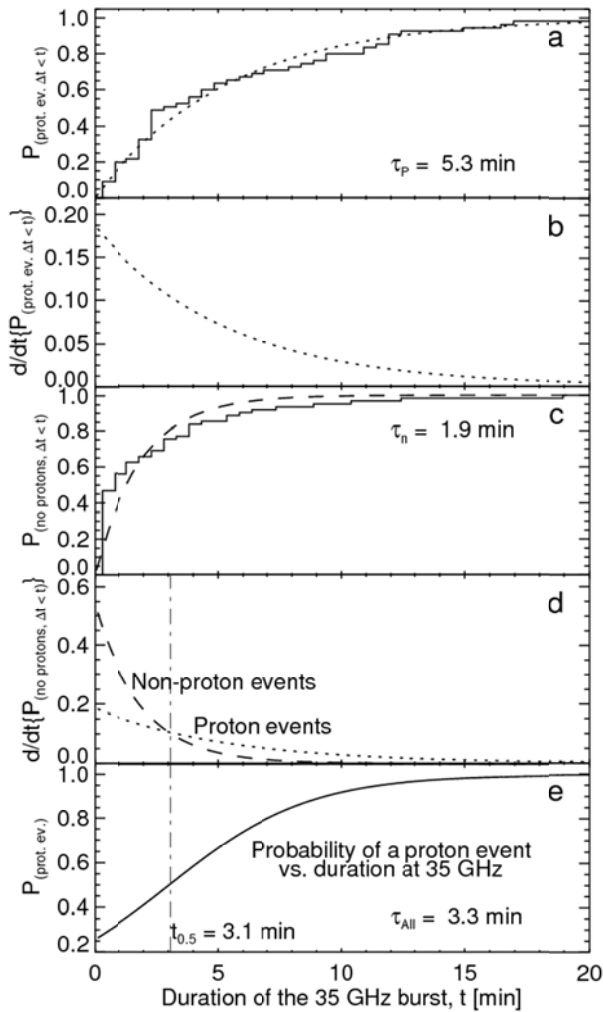

distribution for bursts without SPEs (*c*) and their probability density (*d*). Bottom: SPE probability versus burst duration (*e*)

fit yields τ_p=5.3 min, which characterizes the duration distribution of SPE-related microwave bursts. The corresponding fitting functions are shown by dotted curves in Figure 3, *a* and *b*.

The character of the duration distribution for non-proton events at 35 GHz is the same, but with a lesser width τ_n=1.9 min (Figure 3, *c*, *d*). The fitting functions are shown by the dashed lines. For comparison, the dotted curve in Figure 3, *d* represents the fit of the probability density distribution for SPEs. The ratio of widths of distributions for proton and non-proton events, τ_p / τ_n=2.8, is close to the ratio of their actual average durations of 3.3.

The calculated ratio of the probabilities of proton and non-proton events in Figure 3, *d*, is

$$\frac{P_p}{P_n} = \frac{1-\exp(-t_{35}/\tau_p)}{1-\exp(-t_{35}/\tau_n)}.$$

If the duration of a microwave burst t_{35} is known, the SPE probability $P_p(t_{35})$ can be estimated as:

$$P_p(t_{35}) = \frac{1}{P_p/P_n+1} = \left(\frac{1-\exp(-t_{35}/\tau_p)}{1-\exp(-t_{35}/\tau_n)}+1 \right)^{-1}.$$

With the parameters found for the analyzed set of events, this estimate is 59 %. In fact, SPEs occurred after 60 of 124 microwave bursts with $F_{35} \geq 10^3$ sfu, i.e. in $\approx$ 48 % of the events. The calculated probability for SPEs is shown in Figure 3, *e*. The dash-dotted line in Figure 3, *d*, *e* denotes the burst duration of 3.1 min at which distribution functions of proton and non-proton events are equal. This corresponds to a probability of 0.5. Referring to Figure 3, *e*, if the peak flux of the 35 GHz burst exceeds 1000 sfu and its duration exceeds 15 min, then the SPE probability is close to 100 %.

The fact that the distribution functions for proton and non-proton events are identical in nature indicates that the 35 GHz burst duration itself does not determine the proton productivity of a flare. The whole set of microwave bursts, including both proton and non-proton events, has the same duration distribution. In this case, τ_{total}=3.3 min. This distribution has nothing to do with the proton productivity of the events, being an intrinsic characteristic of microwave bursts. A probable reason for different widths of the distributions, τ_p and τ_n, is the sensitivity of the detector that measures the proton flux in Earth's orbit against the radiation background. A proton bunch injected near the Sun propagating in the interplanetary space undergoes velocity dispersion and other propagation effects, which decrease its peak value. The decrease in the near-Earth SPE peak is especially strong if the bunch has a short duration. Similar reasons might also determine the dependence of the SPE probability on the peak microwave flux shown in Figure 2.

The same shapes of the probability vs. duration distributions suggest that characteristics of 35 GHz bursts do not allow classifying SPEs into "impulsive" and "gradual". Hence, a reason for the dependence of the number of high-energy protons on the duration of an event may be the duration of the acceleration process

Figure 3. Probability of SPE versus duration of a microwave burst at 35 GHz: the integral probability distribution for the duration of SPE-related microwave bursts (*a*) and their probability density (*b*); the integral probability

rather than the difference in particle acceleration mechanisms.

2.3. Proton and microwave fluences

The relationships between various combinations of peak fluxes and fluences of microwave bursts and those of SPEs are presented by four plots in Figure 4. Correlation coefficients for all the events and separately for western events are shown at tops of the plots.

The difference between the top and bottom left panels is insignificant. The five abundant events deviate from the main cloud of points considerably less on the right panels, where the argument is the microwave fluence, than on the left panels, where the argument is the peak microwave flux. The best correspondence with the correlation coefficient of 0.64 is observed between the proton and microwave fluences.

The five mM events (black diamonds) selected according to our criterion exhibit enhanced fluxes of high-energy protons. Perhaps, these events significantly differ from the others. Referring to Figure 4, the highest correlation between the proton and microwave fluences is associated with the long duration of these events; the duration of events with $J_{100} \geq 0.1$ pfu and small bursts at 35 GHz is also long. However, even these events with weak peak proton fluxes on the fluence plot are at the upper boundary of the main sequence. For the events with $F_{35} \geq 1000$ sfu (excluding the mM events), the correlation coefficient between the fluences is 0.81; for the other combinations it does not exceed 0.75.

The linear regression equation obtained for logarithms of proton and microwave fluences in all the events takes the form: $\Phi_{100} = 10^{-0.9 \pm 1.19} \Phi_{35}^{0.96 \pm 0.19}$. The exponent within the scatter is close to unity, which corresponds to the direct proportionality between the fluences. Without the mM events with $F_{35} < 1000$ sfu, the exponent is higher than unity: $\Phi_{100} = 10^{-3.54 \pm 0.98} \Phi_{35}^{1.35 \pm 0.16}$.

The correspondence between the durations of flare acceleration process and microwave burst is obvious. It is, however, more difficult to expect this correspondence if protons are accelerated by shock waves far away from a flare region. This result indicates a statistical predominance of flare-accelerated protons in the energy range of >100 MeV, with the contribution of shock-accelerated protons but with a lower statistical significance. This contradicts the hypothesis of the exceptional shock-acceleration of protons [Kahler, 1982; Reames, 2013; Gopalswamy et al., 2014; Desai, Giacalone, 2016]. To confirm our conclusion, we analyze the correlations of proton fluences with some parameters of flare emission and CME speed.
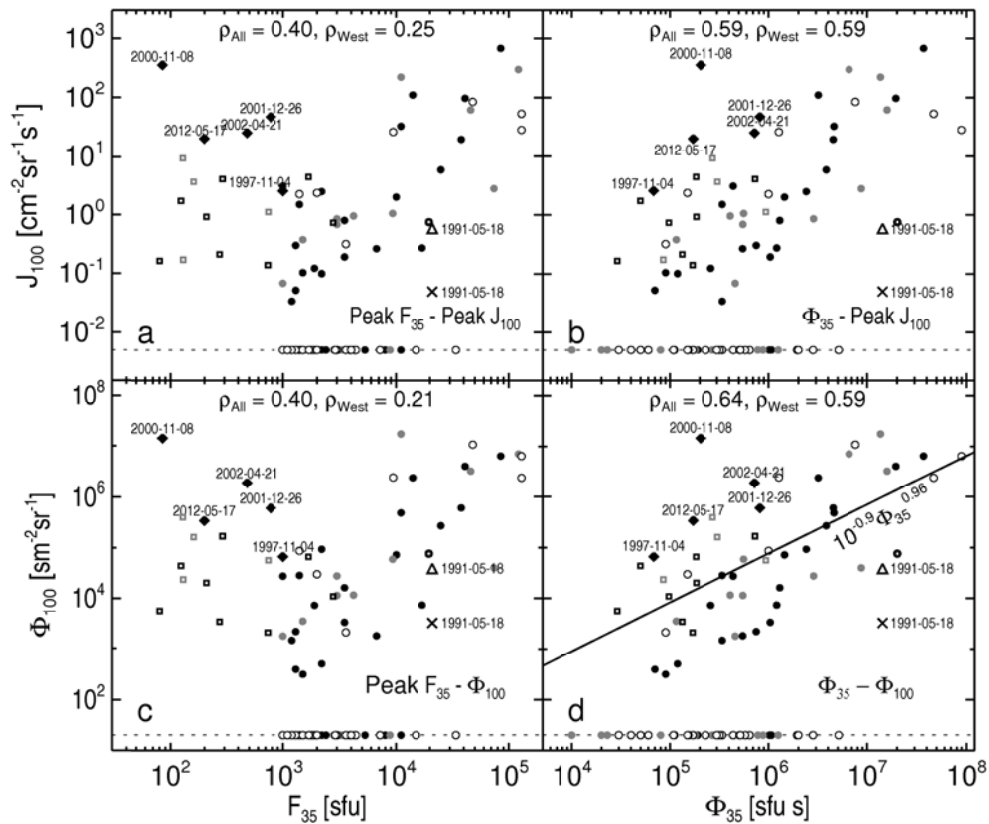

Figure 4. Relationships between different combinations of peak microwave fluxes and fluences at 35 GHz and those of SPEs >100 MeV: peak proton fluxes J_{100} vs. microwave fluxes F_{35} (*a*) and fluences Φ_{35}(*b*); proton fluences Φ_{100} versus microwave fluxes F_{35} (*c*) and fluences Φ_{35} (*d*). At the top are correlation coefficients for all the events and separately for western events. The longitude of the solar source of each event is represented by the color of symbols as in Figure 1. Squares mark 13 events with $0.1 \leq J_{100} < 10$ pfu and $F_{35} < 1000$ sfu. Black diamonds are five atypical proton-abundant mM events. Events without SPEs are shown schematically on the horizontal

dotted line. The solid slanted line in panel *d* is the linear fit of the distribution on the log scale
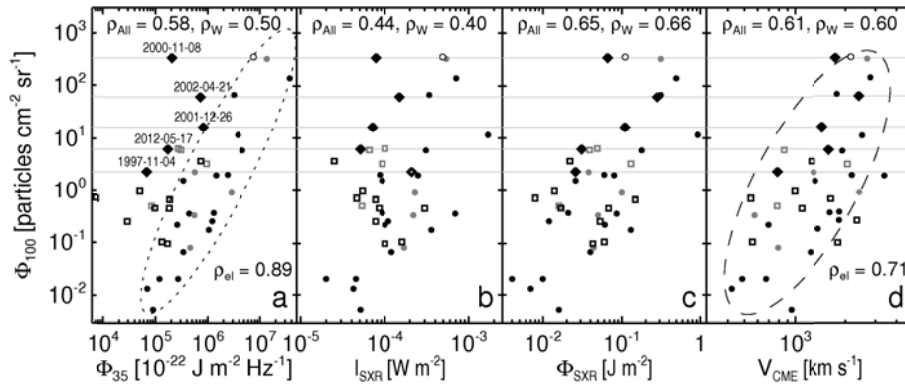

Figure 5. Logarithmic scatter plots for >100 MeV longitude-corrected proton fluences versus different parameters of solar flares and CME speed. At the top of the plots are correlation coefficients for all events (ρ_{All}) and separately for western events (ρ_W). The meaning of the symbols is the same as in Figure 1. Gray horizontal lines trace fluences in the abundant events. Ellipses enclose the events with $F_{35} \geq 1000$ sfu (*a*) and the main cloud of points (*d*); ρ_{el} are the correlation coefficients for events inside the ellipses

3.   RELATIONSHIP BETWEEN PROTON FLUENCES AND PARAMETERS OF ERUPTIVE SOLAR ACTIVITY

Trottet et al. (2015) have analyzed 44 near-Earth SPEs in an energy range 15–40 MeV (and respective fluxes of subrelativistic electrons) associated with M and X-class flares that occurred in the western solar hemisphere in 1997–2006. The authors calculated correlation coefficients between the logarithms of peak proton fluxes and the parameters characterizing flares and CMEs: peak SXR flux, start-to-peak SXR fluence, microwave fluence, and CME speed.

In the proton energy range 15–40 MeV analyzed by Trottet et al., it is difficult to filter out the contribution of interplanetary-shock-related acceleration far from the Sun. It is most likely to be much lower for proton energies above 100 MeV. Figure 4 shows that the microwave fluence Φ_{35} correlates with the total proton fluence Φ_{100} significantly better than with the peak proton flux J_{100}. Therefore, we examine the correlations with total fluences of SPEs and not with their peak fluxes.

Systematic information about CMEs and their speeds for events since 1996 is available in the CME catalog [Yashiro et al., 2004; http://cdaw.gsfc.nasa.gov/ CME_list]. The speeds listed in the CME catalog are measured for the fastest feature, and therefore velocities for fast CMEs are most likely related directly to shock waves [Ciaravella, 2006; Grechnev et al., 2013a, 2014, 2015b; Kwon et al., 2014, 2015]. CME speeds are known for 39 SPEs from our list. Figure 5 presents logarithmic scatter plots for longitude-corrected proton fluences >100 MeV Φ_{100} versus microwave fluences Φ_{35} (Figure 5, *a*), peak SXR fluxes I_{SXR} (Figure 5, *b*), start-to-peak SXR fluences Φ_{SXR} (Figure 5, *c*), and CME speeds V_{CME} (Figure 5, *d*). As in the similar Figure in [Grechnev et al., 2015a], the ellipse in Figure 5, *a* encloses all events with $F_{35} \geq 1000$ sfu (mS and mX); and in Figure 5, *d*, the main cloud of points, which now in-

cludes almost all the events more or less evenly distributed inside the ellipse. The plotted correlation coefficients are essential rather than the ratios of axes of the ellipses depending on scales of coordinate axes.

The analysis of the extended set of events confirms the results and assumptions made in our previous work [Grechnev et al., 2015a]. Events with powerful mS and mX microwave bursts are grouped into a cloud of points with a high correlation of 0.89 between Φ_{100} and Φ_{35} (for the western events inside the ellipse, the correlation coefficient is 0.88). The higher correlation of the proton fluence Φ_{100} with the SXR fluence Φ_{SXR} than with its peak value I_{SXR} is consistent with the fact that the total number of accelerated particles is determined both by the intensity of acceleration process and by its duration. The wider scatter for peak values is most likely determined largely by the effects of proton propagation from a source to near-Earth space.

Data from GOES proton monitors suggest that the increased values of proton fluences for the newly considered events with $0.1 \leq J_{100} < 10$ pfu, the sources of most of which were located in the western hemisphere, are associated with their long duration. Referring to Figure 5, *a*, the 1997 November 4 SPE is also an abundant event associated with a short (0.9 min) microwave burst of 1000 sfu threshold intensity and relatively slow CME (785 km/s), but its proton fluence is atypically high. The probable frequency of the spectral peak of the burst was between 10 and 20 GHz. In its SXR peak flux of X2.1, this event is not atypical; according to its SXR fluence and CME speed, it resides in the upper part of the main cloud of points.

It is reasonable to assume that the contribution of shock-accelerated protons prevailed in the proton-abundant events. It is also possible that some additional factors increasing their proton yield were implicated, especially for the 2000 November 08 event, which stands out in Figure 5, *d* because of its abundant proton fluence, although the speed of respective CME (1738 km/s) was not extreme.

The reported results refer to the total proton fluences integrated over the entire time of the corresponding SPEs. On the other hand, similar studies often deal with proton fluences only during the rise phase of a proton event, in particular to extract its first "fast" component whose connection with flare processes seems more obvious. For completeness, we have also analyzed the same statistical relationships for start-to-peak proton fluences. The correlation coefficients with all the parameters considered turned out to be almost the same as those for total fluences, with differences within 0.02.

4. DISCUSSION AND CONCLUSIONS

Our analysis has revealed relationships between the intensity and duration of microwave bursts recorded at 35 GHz and the probability of SPEs with energies above 100 MeV. The causes of these relationships are most likely associated with the effects of proton propagation from their solar sources to Earth, as well as with the limited sensitivity of detectors. This circumstance suggests the possibility that protons are accelerated to high energies in all flares accompanied by sufficiently strong bursts at 35 GHz, i.e. whenever a great number of electrons are accelerated to relativistic energies. This confirms the conclusions drawn by Livshits and Belov [2004] about the simultaneous acceleration of electrons and protons.

Our results agree with the main conclusion made by Trottet et al. [2015] and confirm their preliminary conclusion that flare acceleration prevails in high-energy protons. For the vast majority of the analyzed events, we have found a direct dependence with a high correlation between flare parameters and fluences of protons with energies above 100 MeV. The comparable correlation of proton fluences with start-to-peak SXR fluences and microwave emission show that both these parameters characterizing solar flares can be used for SPE diagnostics.

Events with sufficiently powerful microwave bursts (F_{35}>1000 sfu) exhibit a high correlation (about 0.9) between microwave and proton fluences, which holds over three orders of magnitude for microwaves and five orders of magnitude for proton events. This corresponds to the power law whose exponent can be roughly estimated as a logarithmic ratio of these ranges, i.e. $5/3 \approx 1.7$. The exponent obtained by linear regression on the log scale is 1.35 ± 0.16. This allows one to estimate practically the expected SPE fluence from the observed microwave burst.

With weaker bursts, the correlation is expected to decrease because only the eruption of a magnetoplasma structure with a strong acceleration is required for the appearance of a shock wave capable of accelerating protons. This can occur without pronounced flare processes responsible for particle acceleration (see, for example, [Grechnev et al., 2015a, b]); such events feature soft spectrum of SPEs [Chertok et al., 2009; Gopalswamy et al., 2015]. The correlation with proton fluences decreases in events with weaker microwave bursts, although not as much as expected: one third of their total number in Figure 5, *a* is inside the correlation ellipse or at its boundary.

Proton-abundant events deserve separate discussion (black diamonds in Figure 5). Differing in some characteristics from other events, the 2000 November 8 event is so far from the correlation ellipse that in our analysis its atypical character can be attributed only to the shock-related acceleration. The very short-duration impulsive event on 1997 November 4 does not fit into the hypothesis of gradual events with supposedly predominant acceleration of protons by shock waves.

The three remaining SPEs, two of which caused GLEs, feature moderate microwave bursts from 200 to 800 sfu with a wide range of durations from 13 to 58 min and spectral peak frequencies not exceeding 10 GHz [Grechnev et al., 2013b]. The existence of events with atypically high proton yield and low frequency of spectral peak has been noticed previously [Melnikov et al., 1991; Daibog et al., 1993]. The detailed analysis of the 2001 December 26 flare has revealed a strong asymmetry in the magnetic configuration. For the magnetic flux to be balanced, the area of the microwave source in weak fields should be larger than that in strong fields with respect to the ratio of their strengths. This leads to an increase in the low-frequency part of the gyrosynchrotron emission spectrum and to a leftward shift of its peak. The strong dependence of the gyrosynchrotron emission on the magnetic field strength in the region of its generation produces an additional several-fold scatter of microwave burst parameters for the same acceleration efficiency [Grechnev et al., 2017]. In fact, these circumstances confirm the assumptions made in [Melnikov et al., 1991; Daibog et al., 1993] about the role of magnetic fields. These effects in the diagnostics can be partially compensated using the morphological indication of the intersection of flare ribbons with sunspot umbras. The most powerful microwave burst occurs if the ribbons cross the umbrae of both sunspots with opposite polarity (as, for example, for GLE69 and GLE70). Bursts with smaller peak fluxes occur when one of the ribbons crosses a sunspot umbra, as was observed in the events that caused GLE63 and GLE71. Moderate bursts occur in most events when the ribbons are outside sunspots.

Another reason for the enhanced proton yield of these three events could be due to the fact that in each of them at least two eruptions occurred within a short time interval. If more than one eruption occurs in the event, the first eruption facilitates the lift-off of the subsequent CME, a higher speed, and excitation of a stronger shock wave. If two shock waves are excited by the eruptions, they merge into a single stronger shock wave. The first eruption releases suprathermal particles that can be accelerated by a shock wave generated by the second eruption. On the other hand, the first eruption stretches closed coronal structures, thus greatly facilitating the release of protons and heavier ions accelerated by flare flare processes in the active region [Grechnev et al., 2013a].

A limitation of our analysis is that the 35 GHz emission in use, which adequately reflects the processes of powerful energy release and particle acceleration during the main phase of the flare, provides insufficient infor-

mation about possible post-eruptive (post-impulsive) particle acceleration with much lower intensity but longer duration. As is known, the peak of the microwave emission spectrum shifts with time to a low-frequency region (which corresponds to the displacement of the microwave source to the region of weak magnetic fields), therefore the prolonged post-eruptive phase appears only at lower frequencies [Chertok, 1995; Klein et al., 1999, 2014]. Hence, the correlation coefficients found for the 35 GHz frequency represent the lower boundary of possible values. The way to take into account possible post-eruptive processes is not yet obvious.

REFERENCES

Akin'yan S.T., Fomichev V.V., Chertok I.M. Estimates of solar proton flux intensity from integral parameters of microwave radio bursts. *Geomagnetizm i Aeronomiya* [Geomagnetism and Aeronomy]. 1978, vol. 18, pp. 577–582. (In Russian).

Aschwanden M.J. GeV particle acceleration in solar flares and ground level enhancement (GLE) events. *Space Sci. Rev.* 2012, vol. 171, iss. 1–4, pp. 3–21. DOI: 10.1007/s11214–011–9865–x.

Bazilevskaya G.A. On the early phase of relativistic solar particle events: are there signatures of acceleration mechanism? *Adv. Space Res.* 2009, vol. 43, pp. 530–536. DOI: 10.1016/j.asr.2008.08.005.

Belov A. Properties of solar X-ray flares and proton event forecasting. *Adv. Space Res.* 2009, vol. 43, iss. 4, pp. 467–473. DOI: 10.1016//j.asr.2008.08.011.

Chertok I.M. On the correlation between the solar gamma-ray line emission, radio bursts and proton fluxes in the interplanetary space. *Astron. Nachr.* 1990, vol. 311, pp. 379–381. DOI: 10.1002/asna.2113110618.

Chertok I.M. Post-eruption particle acceleration in the corona: a possible contribution to solar cosmic rays. *24th International Cosmic Ray Conference*. 1995, vol. 4, p. 78.

Chertok I.M., Grechnev V.V., Meshalkina N.S. On the relationship between spectra of solar and microwave bursts and near-Earth proton fluxes. *Astronomy Reports.* 2009, vol. 53, no. 11, pp. 1059–1069.

Cliver E.W., Forrest D.J., Cane H.V., et al. Solar flare nuclear gamma-rays and interplanetary proton events. *Astrophys. J.* 1989, vol. 343, pp. 953–970. DOI: 10.1086/167765.

Croom D.L. Solar microwave bursts as indicators of the occurrence of solar proton emission. *Solar Phys.* 1971, vol. 19, pp. 152–170. DOI: 10.1007/BF00148831.

Daibog E.I., Kurt V.G., Logachev Yu.I., Stolpovsky V.G., Zenchenko V.N., Melnikov V.F. Yield of electrons generated in solar flares. *Izvestiya AN SSSR. Seriya fizicheskaya* [Bull. of the Russian Academy of Sciences. Physics]. 1987, vol. 51, no. 10, pp. 1825–1827. (In Russian).

Daibog E.I., Melnikov V.F., Stolpovskii V.G. Solar energetic particle events from solar flares with weak impulsive phases of microwave emission. *Solar Phys.* 1993, vol. 144, pp. 361–372. DOI: 10.1007/BF00627600.

Desai, M., Giacalone J. Large gradual solar energetic particle events. *Living Rev. Solar Phys.* 2016, vol. 13, pp. 3–132. DOI: 10.1007/s41116–016–0002–5.

Dierckxsens M., Tziotziou K., Dalla S., et al. Relationship between solar energetic particles and properties of flares and CMEs: statistical analysis of solar cycle 23 events. *Solar Phys.* 2015, vol. 290, pp. 841–874. DOI: 10.1007/s11207–014–0641–4.

Gopalswamy N., Xie H., Akiyama S., et al. Major solar eruptions and high-energy particle events during solar cycle 24. *Earth, Planets and Space.* 2014, vol. 66, article id. 104, 15 p. DOI: 10.1186/1880–5981–66–104.

Gopalswamy N., Mäkelä P.A., Akiyama S., et al. Large solar energetic particle events associated with filament eruptions outside of active regions. *Astrophys. J.* 2015, vol. 806, iss. 1, article id. 8, 15 p. DOI: 10.1088/0004–637X/806/1/8.

Grechnev V.V., Kurt V.G., Chertok I.M., Uralov A.M., Nakajima H., Altyntsev A.T., Belov A.V., Yushkov B.Yu, Kuznetsov S.N., Kashapova L.K., Meshalkina N.S., Prestage N.P. An extreme solar event of 20 January 2005: properties of the flare and the origin of energetic particles. *Solar Phys.* 2008, vol. 252, pp. 149–177. DOI: 10.1007/s11207–008–9245–1.

Grechnev V.V., Kiselev V.I., Uralov A.M., et al. An updated view of the solar eruptive flares and the development of shocks and CMEs: history of the 2006 December 13 GLE-productive extreme event. *Publ. Astron. Soc. Japan.* 2013a, vol. 65, SP1, S9. DOI: 10.1093/pasj/65.sp1.S9.

Grechnev V.V., Meshalkina N.S., Chertok I.M., Kiselev V.I. Relations between strong high-frequency microwave bursts and proton events. *Publ. Astron. Soc. Japan.* 2013b, vol. 65, SP1, S4. DOI: 10.1093/pasj/65.sp1.S4.

Grechnev V.V., Kiselev V.I., Meshalkina N.S., Chertok I.M. Relations between microwave bursts and near-Earth high-energy proton enhancements and their origin. *Solar Phys.* 2015a, vol. 290, iss. 10, pp. 2827–2855. DOI: 10.1007/s11207–015–0797–6.

Grechnev V.V., Uralov A.M., Kuzmenko I.V., Kochanov A.A., Chertok I.M., Kalashnikov S.S. Responsibility of a filament eruption for the initiation of a flare, CME, and blast wave, and its possible transformation into a bow shock. *Solar Phys.* 2015b, vol. 290, iss. 1, pp. 129–158. DOI: 10.1007/s 11207–014–0621–8.

Grechnev V.V., Uralov A.M., Kiselev V.I., Kochanov A.A. The 26 December 2001 solar eruptive event responsible for GLE63. II. Multi-loop structure of microwave sources in a major long-duration flare. *Solar Phys.* 2017, vol. 292, iss. 1, article id. 3, 27 p. DOI: 10.1007/s11207–016–1025–8.

Isaeva E.A., Melnikov V.F., Tsvetkov L.I. Dependence of the SCR proton flux estimate on radio burst parameters. *Bull. Crimean Astrophys. Obs.* 2010, vol. 106, pp. 26–30. DOI: 10.3103/S0190271710010043.

Kahler S.W. The role of the big flare syndrome in correlations of solar energetic proton fluxes and associated microwave burst parameters. *J. Geophys. Res.* 1982, vol. 87, pp. 3439–3448. DOI: 10.1029/JA087iA05p03439.

Kallenrode M.-B. Current views on impulsive and gradual solar energetic particle events. *J. Phys. G.* 2003, vol. 29, iss. 5, pp. 965–981.

Klein K.-L., Chupp E.L., Trottet G., Magun A., Dunphy P.P., Rieger E., Urpo S. Flare-associated energetic particles in the corona and at 1 AU. *Astron. Astrophys.* 1999, vol. 348, pp. 271–285.

Klein K.-L., Masson S., Bouratzis C., et al. The relativistic solar particle of 2005 January 20: origin of delayed particle acceleration. *Astron. Astrophys.* 2014, vol. 572, id. A4, 8 p. DOI: 10.1051/0004–6361/201423783.

Lario D., Aran A., Decker R.B. Major solar energetic particle events of solar cycles 22 and 23: intensities close to the streaming limit. *Solar Phys.* 2009, vol. 260, iss. 2, pp. 407–421. DOI: 10.1007/s11207–009–9463–1.

Lario D., Aran A., Gómez-Herrero R., et al. Longitudinal

and radial dependence of solar energetic particle peak intensities: STEREO, ACE, SOHO, GOES, and MESSENGER observations. *Astrophys. J.* 2013, vol. 767, pp. 41–59. DOI: 10.1088/0004–637X/767/1/41.

Livshits M.A., Belov A.V. When and where are solar cosmic rays accelerated most efficiently? *Astron. Rep.* 2004, vol. 48, pp. 665–677. DOI: 10.1134/1.1787069.

Logachev Yu.I., Bazilevskaya G.A., Vashenyuk E.V., et al. *Catalogue of Solar Proton Events in the 23ʳᵈ Cycle of Solar Activity (1996–2008).* Moscow, Geophysical Center RAS Publ., 2016, 740 p. DOI: 10.2205/ ESDB–SAD–P–001.

Melnikov V.F., Podstrigach T.S., Dajbog E.I., Stolpovskij V.G. Nature of the relationship between the fluxes of solar cosmic ray electrons and protons and the parameters of microwave bursts. *Cosm. Res.* 1991, vol. 29, no. 1, pp. 87–94.

Miroshnichenko L.I., Vashenyuk E.V., Perez-Péraza J. Solar cosmic rays: 70 years of ground-based observation. *Geomagnetizm i aeronomiya* [Geomagnetism and Aeronomy]. 2013, vol. 53, no. 5, pp. 579–600. DOI: 10.7868/S00167 9401305012X. (In Russian).

Nakajima H., Sekiguchi H., Sawa M., et al. The radiometer and polarimeters at 80, 35, and 17 GHz for solar observations at Nobeyama. *Publ. Astron. Soc. of Japan.* 1985, vol. 37, no. 1, pp. 163–170.

Reames D.V. Solar release times of energetic particles in ground-level events. *Astrophys. J.* 2009, vol. 693, pp. 812–821. DOI: 10.1088/0004–637X/693/1/812.

Reames D.V. The two sources of solar energetic particles. *Space Sci. Rev.* 2013, vol. 175, iss. 1–4, pp. 53–92. DOI: 10.1007/ s11214–013–9958–9.

Sladkova A.I., Bazilevskaya G.A., Ishkov V.N., et al. *Catalogue of Solar Proton Events 1987–1996.* Moscow, Moscow University Press, 1998, 247 p.

Trottet G. E., Samwel S., Klein K.-L., et al. Statistical evidence for contributions of flares and coronal mass ejections to major solar energetic particle events. *Solar Phys.* 2015, vol. 290, iss. 3, pp. 819–839. DOI: 10.1007/s11207–014–0628–1.

Veselovsky I.S., Panasyuk M.I., Avdyushin S.I., Bazilevskaya G.A. Solar and heliospheric events in Octo November 2003: causes and effects. *Kosmicheskie issledova* [Cosmic Research]. 2004, vol. 42, pp. 435–488. L 10.1023/B: COSM.0000046229.24716.02. (In Russian).

Veselovsky I.S., Myagkova I.N., Yakovchuk O.S. Dynamics of energetic spectra of solar proton events in 23 solar cycle. *Astronomicheskii vestnik* [Astron. Bull.]. 2012, vol. 46, no. 3, pp. 235–258. DOI: 10.1134/S0038094612030033. (In Russian).

URL: http://solar.nro.nao.ac.jp/norp/html/event (accessed March 10, 2017).

URL: ftp://ftp.swpc.noaa.gov/pub/warehouse (accessed March 10, 2017).

URL: http://www.wdcb.ru/stp/data/SPE (accessed March 10, 2017).

URL: http://solar.nro.nao.ac.jp/norh (accessed March 10, 2017).

URL: http://cdaw.gsfc.nasa.gov/CME_list (accessed March 10, 2017).

URL: http://lasco-www.nrl.navy.mil/daily_mpg (accessed March 10, 2017).

URL: http://cdaw.gsfc.nasa.gov/stereo/daily_movies (accessed March 10, 2017).

URL: http://sdo.gsfc.nasa.gov/data/aiahmi (accessed March 10, 2017).

URL: http://iszf.irk.ru/~grechnev/papers/protons_microwaves/Table.htm (accessed March 10, 2017).

URL: ftp://solar-pub.nao.ac.jp/pub/nsro/norp/xdr (accessed March 10, 2017).

URL: http://satdat.ngdc.noaa.gov/sem/goes/data/new_avg (accessed March 10, 2017).